A Mode-Matching Technique for Mode Coupling in a Gyrotron Cavity

Vasu Kasibhotla, *Student Member, IEEE*, and Alan H. McCurdy, *Member, IEEE*

Abstract— **The mode-matching technique (MMT) is used to compute the electromagnetic fields, stored energy, and input admittances of a gyrotron cavity coupled to one or more waveguides. The method is based on matching the cavity and waveguide eigenmodes across the cavity apertures and accommodates cavity walls of finite conductivity. The MMT is used in the gyrotron problem because fields in and near the aperture must be computed accurately, and because the eigenmode decomposition is advantageous for inclusion of an electron beam. Irrotational modes are part of the complete set of orthogonal vectors required to expand an H-field in an open cavity, but were excluded in most gyrotron literature; here, this is corrected. The MMT is numerically implemented for cavities of rectangular and circular cross section. Coupling between different modes in a gyrotron cavity through external and ohmic losses is demonstrated. A coupled (complex) cavity gyrotron design is analyzed using MMT. The energy and modal spectra of the cavity are computed, demonstrating the mode selective properties of the design.**

I. Introduction

IN A GYROTRON or other high power microwave oscillator operating at high frequencies, it is not uncommon to have two or more cavity electromagnetic modes in competition. It is important in such situations to be able to describe the coupling between different modes accurately. In addition to coupling through the electron beam, mode coupling can occur through both external and ohmic losses in the cavity. Typically, the gyrotron cavity is strongly coupled to the output via an oversized waveguide, and this usually results in mode coupling through external losses. In practice, the cavity wall conductivity is usually high, but when modes are closely spaced in frequency there may be some coupling through ohmic losses in the cavity surface. New equations and results that include ohmic cross-coupling effects through the cavity walls are presented. In addition, irrotational modes that must be included to get the correct expansion for the H-field in a cavity with apertures in the cavity walls were not inluded in much of the gyrotron literature. In this work, these irrotational modes are included.

A number of techniques are available to describe the cavity field excitation via the waveguide. They include the variational method [1], the mode-matching technique (MMT) [2]–[4], the method of moments (MOM) [5]–[7], and the scattering matrix method [10], [11]. The variational methods yield accurate results for single mode propagation but ignore higher order mode interactions. The MMT is based on matching the waveguide and cavity modes at the junction. The MOM analysis provides accurate results for waveguide discontinuities, and has proven to be more computationally efficient than MMT in some cases. The scattering matrix method [11] has proven to be useful in determining the quality factors and resonant frequencies of a complex cavity.

The size of the scattering matrix in MOM [5] is proportional to the number of the interacting modes (propagating and weakly evanescent); however, the number of modes required to compute the field intensity in or near the plane of discontinuity is on the same order as the mode-matching technique. To describe the interaction of the gyrotron electron beam with the cavity fields, it is required that fields in the cavity-waveguide junction be computed accurately. Many evanescent modes are present near the waveguide-cavity junction. It is important to be able to accurately determine the amplitude of these evanescent waveguide modes in the plane of discontinuity, as the amplitudes of cavity eigenmodes are determined by the tangential electric field in the cavity-waveguide junction. Moreover, in gyrotron theory, it is convenient to be able to predict the growth of individual cavity modes with the beam present, and the usual techniques for computing gyrotron performance are heavily dependent on modal decomposition. For this reason, the MMT is used to describe mode conversion in the gyrotron problem.

The scattering matrix method [10] has been used in the formulation of a problem in which a series of waveguides of different cross sections are connected with either open or closed ends. As with the MOM and MMT methods, to obtain an accurate field representation in the cavity, a large number of waveguide modes are required. The MMT can conveniently include the ohmic effects of cavity walls, beam current loading, and side-wall cavity coupling through terms in the resulting oscillator equations.

A number of early workers developed electromagnetic modal expansions in a conducting cavity [2], [3]. Many of these proved to be either incomplete or difficult to evaluate. The complete sets of orthonormal modes given in [4] are more suitable for a general expansion of electromagnetic fields in a cavity, and are used here.

Here MMT is numerically applied to describe the excitation of electromagnetic fields in a gyrotron cavity coupled to one or more waveguides. Losses due to finite conductivity of the walls are taken into account. The numerical results are benchmarked

Manuscript received November 23, 1994; revised November 12, 1995. This work was supported by the Air Force Office of Scientific Research and National Science Foundation sponsored San Diego Supercomputer Center.

The authors are with the Department of Electrical Engineering—Electrophysics, M.C. 0271, University of Southern California, Los Angeles, CA 90089-0271 USA.

Publisher Item Identifier S 0018-9480(96)01440-8.

against the known analytical solutions for fields in a shorted waveguide and the known ohmic Q and frequency shift of a weakly coupled cavity resonance [2], [8]. Coupling between modes through radiation loss and dissipation in the cavity walls is demonstrated and quantified. The equations developed here can be readily modified to include an electron beam in the gyrotron cavity.

Section II presents a formulation of the MMT as applied to the cavity/waveguide problem including an electron beam. The oscillator equations governing the growth of electromagnetic modes in the gyrotron cavity are derived. A method is described to solve the oscillator equations. Section III gives benchmarks for the numerical results, and discusses application of the theory to both a gyrotron cavity with lossy walls and a coupled (complex) cavity gyrotron. Section IV outlines the conclusions.

II. Analytical Formulation

Fig. 1 shows a circular waveguide exciting a cavity of circular cross section. The electric and magnetic fields in the cavity are expressed as sums of short circuit eigenmodes as

$$\vec{E}_c(\vec{r},t) = \sum_\alpha \vec{E}_\alpha(\vec{r}) \int_V \vec{E}_c(\vec{r},t)\cdot\vec{E}_\alpha(\vec{r})\,dv \tag{1}$$

and

$$\vec{H}_c(\vec{r},t) = \sum_\alpha \vec{H}_\alpha(\vec{r}) \int_V \vec{H}_c(\vec{r},t)\cdot\vec{H}_\alpha(\vec{r})\,dv + \sum_\lambda \vec{G}_\lambda(\vec{r}) \int_V \vec{H}_c(\vec{r},t)\cdot\vec{G}_\lambda(\vec{r})\,dv. \tag{2}$$

Here the $\vec{E}_\alpha$ and $\vec{H}_\alpha$ are the solenoidal modes and $\vec{G}_\lambda$ are the irrotational modes. It is to be noted that the irrotational modes $\vec{G}_\lambda$ are part of the complete set of eigenvectors required in the magnetic field expansion in a cavity which is not completely enclosed by a perfect conductor [4]. Irrotational modes are not required to expand the electric field because all irrotational modes are orthogonal to the real electric field in the absence of an electron beam. (In the presence of an electron beam, irrotational modes can be ignored in the electric field expansion if the space charge effects are neglected.) The eigenmodes satisfy the orthonormality relations given by

$$\int_V \vec{E}_\alpha\cdot\vec{E}_\beta\,dv = \int_V \vec{H}_\alpha\cdot\vec{H}_\beta\,dv = \int_V \vec{G}_\alpha\cdot\vec{G}_\beta\,dv = \delta_{\alpha\beta} \tag{3}$$

where δ is the Kronecker delta function.

Expanding the curl of the electric and magnetic fields in terms of the appropriate eigenmodes and substituting into Maxwell's equations [2], the oscillator equations describing the time evolution of electromagnetic fields in the cavity are obtained as follows

$$\frac{1}{c^2}\frac{d^2}{dt^2}\int_V \vec{E}_c\cdot\vec{E}_\alpha\,dv + k_\alpha^2\int_V \vec{E}_c\cdot\vec{E}_\alpha\,dv = -k_\alpha\int_{S+S'}(\vec{n}\times\vec{E}_c)\cdot\vec{H}_\alpha\,dS - \mu\frac{d}{dt}\int_V \vec{J}\cdot\vec{E}_\alpha\,dv \tag{4}$$

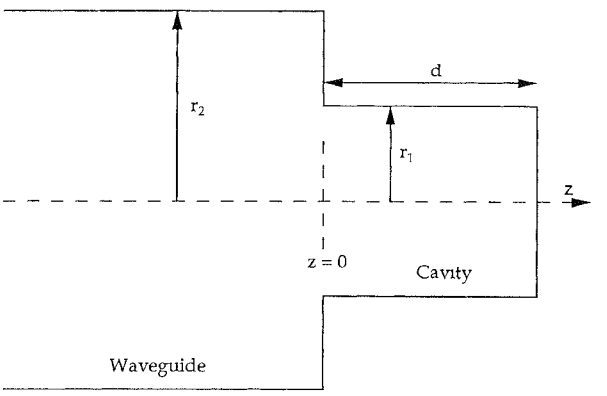

Fig. 1. Cross section of a circular waveguide coupled to a circular cavity.

and

$$\frac{1}{c^2}\frac{d^2}{dt^2}\int_V \vec{H}_c\cdot\vec{H}_\alpha\,dv + k_\alpha^2\int_V \vec{H}_c\cdot\vec{H}_\alpha\,dv = k_\alpha\int_V \vec{J}\cdot\vec{E}_\alpha\,dV - \varepsilon\frac{d}{dt}\int_{S+S'}(\vec{n}\times\vec{E}_c)\cdot\vec{H}_\alpha\,ds \tag{5}$$

where S is the conducting portion of the cavity surface, S' is the open portion of the cavity surface, V is the cavity volume, k_α is the resonant wavenumber, $\vec{n}$ is the outwardly directed unit normal vector at the cavity surface, and $\vec{J}$ is the electron beam current density.

Here the problem is solved in the steady state. The waveguide fields are expressed as sums over the corresponding waveguide eigenmodes as

$$\vec{E}_w(\vec{r}_\perp,z,\omega) = \sum_s v_s(z,\omega)\vec{F}_{t,s}(\vec{r}_\perp + i_s(z,\omega)Z_s(\omega)\vec{F}_{z,s}(\vec{r}_\perp) \tag{6}$$

and

$$\vec{H}_w(\vec{r}_\perp,z,\omega) = \sum_s i_s(z,\omega)\vec{G}_{t,s}(\vec{r}_\perp) + \frac{v_s(z,\omega)}{Z_s(\omega)}\vec{G}_{z,s}(\vec{r}_\perp) \tag{7}$$

where $\vec{F}_{t,s}$ and $\vec{F}_{z,s}$ are the transverse and longitudinal parts of the s'th electric field eigenmode, $\vec{G}_{t,s}$ and $\vec{G}_{z,s}$ are the transverse and longitudinal parts of the s'th magnetic field eigenmode, v_s, i_s, and Z_s are the voltage, current, and impedance associated with mode s, respectively. The waveguide eigenmodes are orthonormalized as

$$\int_{S'}\vec{F}_{tr}\cdot\vec{F}_{ts}ds = \int_{S'}\vec{G}_{tr}\cdot\vec{G}_{ts}\,ds = \int_{S'}(\vec{F}_{tr}\times\vec{G}_{ts})\cdot\vec{z}\,ds = \delta_{rs}. \tag{8}$$

Equations (6) and (7) are applicable to waves propagating in the $+z$ and $-z$ directions in the waveguide. If both forward and backward waves are present, then the voltages and currents are related as

$$v_s = v_s^+ - v_s^- \quad\text{and}\quad i_s = i_s^+ + i_s^-. \tag{9}$$

It is assumed that there is no beam present in the gyrotron cavity. It is also assumed that the waveguide is excited by a source of unit amplitude propagating in the dominant mode

($v_s^+ = 1$ for $s = 1, v_s^+ = 0$ otherwise). Equation (4) is Fourier transformed to obtain

$$f_\alpha(\omega) = \frac{-k_\alpha}{\left(k_\alpha^2 - \frac{\omega^2}{c^2}\right)} \int_{S+S'} \{\vec{n} \times \vec{E}_c(\vec{r}, \omega)\} \cdot \vec{H}_\alpha(\vec{r})\, ds$$

where

$$f_\alpha = \int_V \vec{E}_c \cdot \vec{E}_\alpha\, dv. \tag{10}$$

From Maxwell's equations, the amplitude coefficients of the magnetic field are obtained as

$$h_\alpha(\omega) = \frac{j\omega\varepsilon}{k_\alpha} f_\alpha(\omega)$$

where

$$h_\alpha = \int_V \vec{H}_c \cdot \vec{H}_\alpha\, dv \tag{11}$$

and

$$g_\lambda(\omega) = \frac{-1}{j\omega\mu} \int_{S+S'} \{\vec{n} \times \vec{E}_c(\vec{r}, \omega)\} \cdot \vec{G}_\lambda\, ds$$

where

$$g_\lambda = \int_V \vec{H}_c \cdot \vec{G}_\lambda\, dv. \tag{12}$$

The electric and magnetic fields in the cavity are coupled through the cavity surface impedance $\eta(\omega)$ as

$$\vec{n} \times \vec{E}_c(\omega) = \eta(\omega) \vec{H}_c(\omega) \tag{13}$$

on the conducting portion of the cavity surface. By defining cavity ohmic quality factors as

$$Q_{hh}^{\alpha\beta} = \frac{2}{\delta \int_S \vec{H}_\alpha \cdot \vec{H}_\beta\, ds}, \quad Q_{hg}^{\alpha\beta} = \frac{2}{\delta \int_S \vec{H}_\alpha \cdot \vec{G}_\beta\, ds},$$

and

$$Q_{gg}^{\alpha\beta} = \frac{2}{\delta \int_S \vec{G}_\alpha \cdot \vec{G}_\beta\, ds} \tag{14}$$

where δ is the skin depth (evaluated at $\omega_\alpha; \omega_\alpha = k_\alpha c$), and using (6), (10), and (13), the continuity of electric field across the cavity-waveguide aperture gives

$$f_\alpha = \frac{-k_\alpha \eta(\omega)}{k_\alpha^2 - \frac{\omega^2}{c^2}} \sum_\varphi \frac{j\omega\varepsilon}{k_\varphi} \frac{1}{Q_{hh}^{\alpha\varphi}\delta} f_\varphi + \sum_n \sum_s \frac{k_\alpha}{k_\alpha^2 - \frac{\omega^2}{c^2}} \left[\gamma_\alpha, s_n - \sum_\varphi \frac{\eta(\omega)}{Q_{hg}^{\alpha\varphi}\delta} \frac{\beta_{\varphi,s_n}}{j\omega\mu}\right] v_{s_n}. \tag{15}$$

Here

$$\gamma_{\alpha,s_n} = \int_{S'} \vec{H}_\alpha \cdot \vec{G}_{t,s_n} ds \quad \text{and} \quad \beta_{\lambda,r_n} = \int_{S'} \vec{G}_\lambda \cdot \vec{G}_{t,r_n}\, ds. \tag{16}$$

Similarly, the continuity of the magnetic field across the cavity-waveguide aperture, along with (2), (7), (10), (11), and (13) gives

$$i_{r_m} = \sum_\alpha \left[\gamma_{\alpha,r_m} + j \sum_\lambda \beta_{\lambda,r_m} \frac{\eta(\omega)}{\omega\mu} \frac{1}{Q_{hg}^{\lambda\alpha}\delta}\right] \frac{j\omega\varepsilon}{k_\alpha} f_\alpha + \sum_n \sum_s \left[\left\{\sum_\alpha \sum_\lambda \beta_{\alpha,r_m}\beta_{\lambda,s_n} \frac{\eta(\omega)}{\omega^2\mu^2} \frac{1}{Q_{gg}^{\alpha\lambda}\delta}\right\} - j\left\{\sum_\alpha \frac{\beta_{\alpha,r_m}\beta_{\alpha,s_n}}{\omega\mu}\right\}\right] v_{s_n}. \tag{17}$$

Equations (15), (16), and (17) are written in a generalized way so as to include a case where the cavity is fed by more than one waveguide. The index "n" is over all the waveguides coupled to the cavity, and $\vec{G}_{t,s_n}$ is the transverse part of the s'th magnetic field eigenmode in the n'th waveguide coupled to the cavity. The coefficients γ_{α,s_n} and β_{λ,r_n} give a measure of the coupling between the α'th cavity mode and the s'th mode in the n'th waveguide. γ and β are inversely proportional to the external quality factors Q_e. The ohmic Q factors include both self- and cross-coupling terms. It is to be noted that (15) and (17) are actually power-series expansions in the small quantity $\frac{\eta(\omega)}{\eta_0}$ where $\eta_0 = \sqrt{\frac{\mu}{\varepsilon}}$. For the case of a single cavity mode, (15) reduces to

$$f_\alpha = \frac{\sum_n \sum_s k_\alpha \left[\gamma_{\alpha,s_n} - \frac{\eta(\omega)}{Q_{hg}^{\alpha\alpha}\delta} \frac{\beta_{\alpha,s_n}}{j\omega\mu}\right] v_{s_n}}{\left(k_\alpha^2 - \frac{\omega^2}{c^2}\right) + \frac{j\omega\varepsilon\eta(\omega)}{Q_{hh}^{\alpha\alpha}\delta}}$$

where the typical $\frac{j\omega}{Q}$ ohmic dependence in the denominator is observed. In addition, note the ohmic modification in waveguide-cavity coupling through the $\beta_{\alpha,s}$ term. Equations (15) and (17) can be written in matrix form as

$$(f) = (A)(f) + (B)[(v^+) - (v^-)] \tag{18}$$

and

$$(i) = (C)(f) + (D)[(v^+) - (v^-)]. \tag{19}$$

Further, the waveguide currents and voltages are related through the waveguide modal admittances as

$$i_{m_r} = i_{m_r}^+ + i_{m_r}^- = Y_{\omega_{r_m}}[v_{m_r}^+ + v_{m_r}^-]. \tag{20}$$

In (18)–(20), the total voltage (v) and current (i) in the waveguides have been split into waves traveling toward $(+)$ and away $(-)$ from the cavity. Equations (18)–(20) are solved simultaneously for the cavity field amplitude coefficients. This completes the formulation of the waveguide-cavity coupling problem.

III. Numerical Results

The method described in Section II has been computer coded to compute the admittance matrix coefficients, voltages in the waveguide-cavity aperture, amplitudes of individual cavity modes, cavity fields as a function of incident wave frequency and position in the cavity, and the stored energy in the cavity. The codes were written in a very general way so that they can handle both rectangular and circular geometries.

The code was first benchmarked against known results for shorted rectangular and circular waveguides. Fig. 2 shows the stored energy (obtained as $\sum_\alpha |f_\alpha|^2$) in a circular cavity of perfectly conducting walls as a function of frequency of the incident TE_{01} wave (when the cavity and the feeding waveguide have equal transverse dimensions) compared to the analytical result of a shorted waveguide. (The case of cavity with perfectly conducting walls is solved by using a

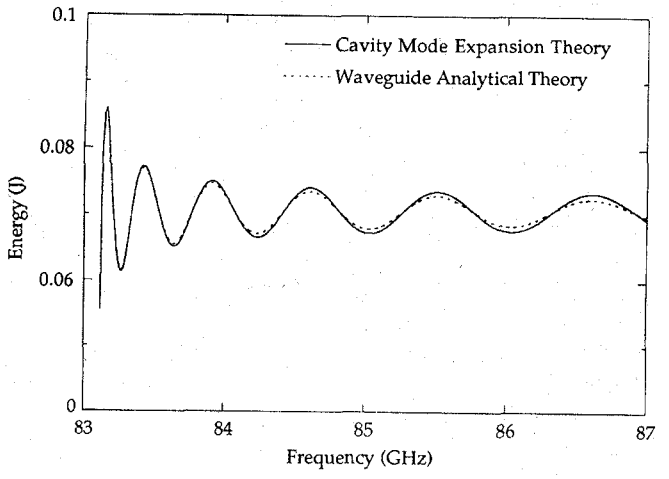

Fig. 2. Energy spectrum for the configuration in Fig. 1 (when waveguide radius equals cavity radius) compared to that of a shorted waveguide. Incident waveguide mode is TE_{01}.

value of infinity for the ohmic Q factors and $\eta(\omega) = 0$.) The waveguide dimensions are chosen to be $r_1 = r_2 = 0.22$ cm, and $d = 3.5$ cm; 290 TE_{01p} cavity modes are used. It is to be noted that this many modes are required only to accurately represent an electric field with an antinode at the aperture. In the frequency range shown in Fig. 2, the energy obtained from the cavity field expansion theory converges to within 2% of the waveguide analytical result. The disagreement between the results increases with frequency. This is because the admittance function expansion at the cavity-waveguide junction has a slower rate of convergence with increasing frequency, when the number of modes is fixed. As can be expected, the convergence improves with an increase in the number of axial modes used. The Q_e are measured from Fig. 2 by measuring the full width at half maximum (FWHM), and are found to be in good agreement with Q_e obtained from the waveguide analytical formula ($Q_e = \frac{\omega_o E}{P_l}$ where E is the energy stored in the cavity and P_l is the radiation power loss). This benchmark provides a test of the coupling between the cavity and the waveguide.

Another benchmark tests the code for the inclusion of the ohmic effects. Here Q_e is made to be of the same order of magnitude as the ohmic quality factor $Q_o, (Q_o = Q_{hh}^{\alpha\alpha})$; by minimizing the external losses, the effect of ohmic losses can be seen more clearly. The rectangular geometry provides a convenient means of increasing the Q_e since the waveguide height can be decreased to reduce the external losses, without a corresponding increase in the waveguide cut-off frequency. Fig. 3 shows the geometry of a rectangular cavity coupled to a rectangular waveguide. The benchmark is run using cavity and waveguide dimensions of $a = 1.783$ cm, $b = 0.993$ cm, $c = b/100$, and $d = 4.0$ cm. The conductivity of the cavity walls is 1.0×10^6 S/m (close to stainless steel). Fig. 4 compares the results for cavities with walls of finite and infinite conductivity. Q_e is measured to be 920 from Fig. 4 from the FWHM of the solid curve. The total quality factor (Q_t) is measured from the FWHM of the dashed curve to be 476. Q_o is computed as $(\frac{1}{Q_o} = \frac{1}{Q_t} - \frac{1}{Q_e})$ and is measured to be 989. This value for Q_o agrees very well with the result for the

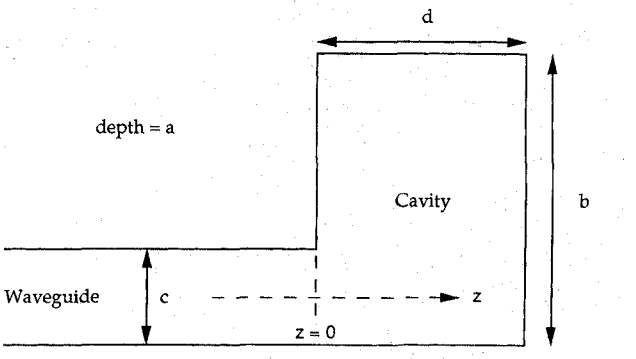

Fig. 3. Cross section of a rectangular waveguide feeding a rectangular cavity.

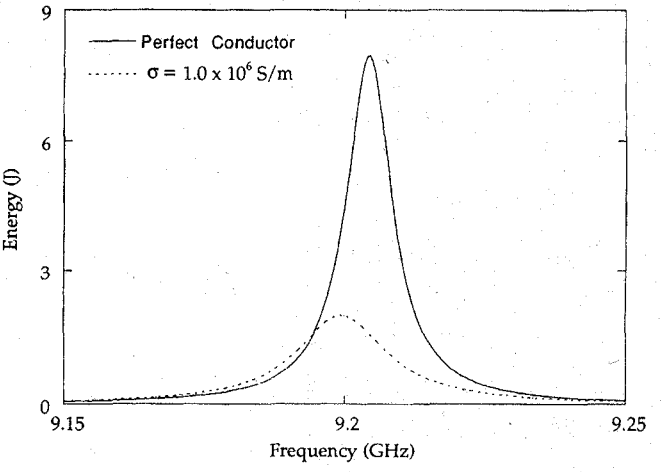

Fig. 4. Comparison of energy spectra for the cavity in Fig. 3 for cases of perfectly and imperfectly conducting walls.

known analytical result for Q_o, computed to be 980 [8]. From Fig. 4, the shift in the resonant frequency between the two energy profiles is measured to be 4.65 MHz, which agrees well with the known analytical shift ($\Delta\omega = \frac{\omega_o}{2Q_o} = 4.69$ MHz) [2].

To demonstrate mode coupling through external and ohmic effects in a gyrotron cavity, the configuration in Fig. 1 is used to excite fields in a cavity of circular cross section. The cavity and waveguide dimensions are $r_1 = 0.22$ cm, $r_2 = 0.25$ cm, and $d = 3.5$ cm. The conductivity of the cavity walls is 1.0×10^6 S/m. These dimensions result in a set of closely spaced TE_{01p} modes. The incident waveguide mode is TE_{01}. Fig. 5 shows the stored energy in cavities of finite and infinite conductivity and the amplitudes of the first four axial modes as a function of frequency in a cavity of finite conductivity. Coupling exists between adjacent modes through both external and ohmic effects. That there is mode coupling can be seen by the stored energy in the cavity (Fig. 5(a)) which does not drop to zero at any frequency, and also from the finite width of the resonances. The lowest order modes have the highest external Q-factors because their resonant frequencies are closest to the cut-off frequency (83.1 GHz), hence resulting in a larger impedance mismatch at the aperture. The ohmic effects are more pronounced for the TE_{011} mode compared to the other cavity modes because there is a larger amount of dissipation in the cavity walls in TE_{011} mode due to its lower group

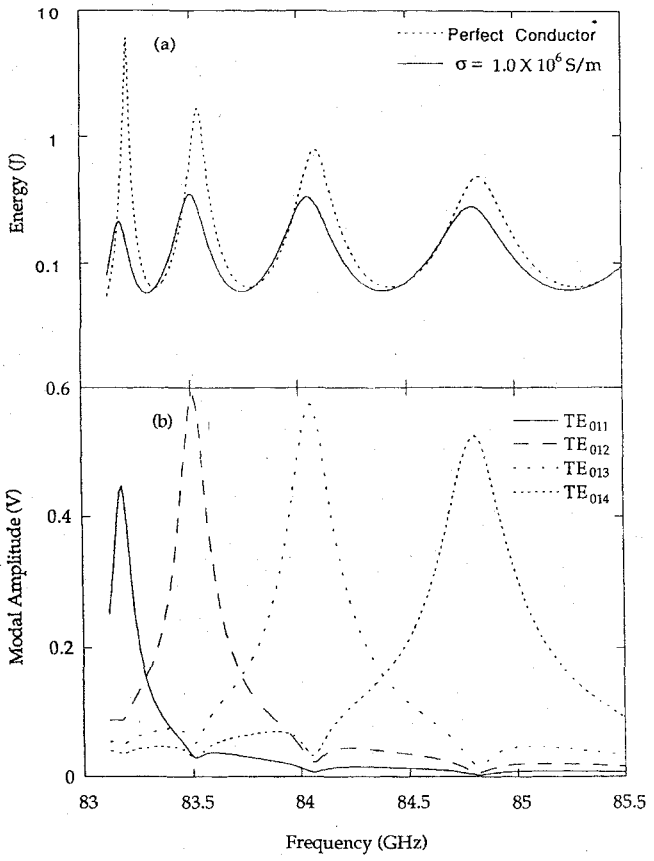

Fig. 5. (a) Top, energy spectra for the cavity in Fig. 1 for cases of finite and perfectly conducting walls, and (b) bottom, profile of the first four modal amplitudes.

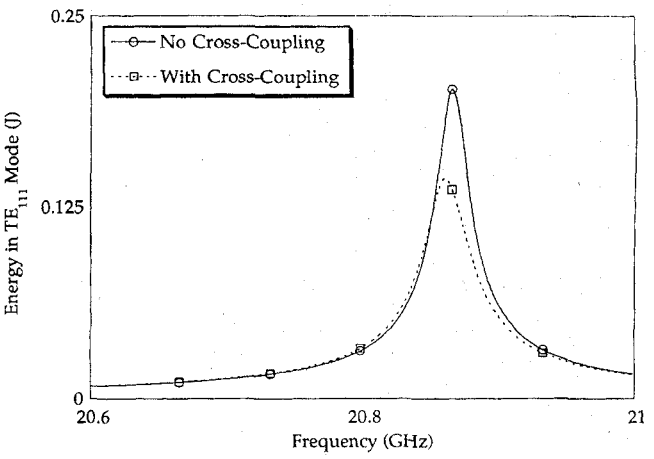

Fig. 6. Comparison of energy in the TE_{111} mode for the cavity in Fig. 3 for cases of no coupling between modes and with and without cross-coupling.

velocity [13]. The maxima of individual modal amplitudes (Fig. 5(b)) occur at approximately the same frequencies as the maxima of the energy profiles, indicating dominance of the corresponding mode at its resonant frequency. Between any two resonant frequencies; however, the corresponding adjacent modes are of the same order of magnitude, indicating strong mode coupling through external losses. The measured external Q factors decrease approximately as $\frac{1}{p^2}$ where p is mode axial number. This is in agreement with known analytical formula [12].

Significant cross-coupling from the α'th cavity mode to the β'th cavity mode occurs through the ohmic losses only if: 1) $\frac{f_\beta}{Q_{hh}^{\beta\beta}}$ and $\frac{f_\alpha}{Q_{hh}^{\beta\alpha}}$ are of the same order of magnitude and 2) ω_α and ω_β are nearly equal. From the expressions for ohmic Q-factors for the cavity in Fig. 1 (see Appendix), it can be seen that in an azimuthally symmetric cavity, cross-coupling can occur only if the azimuthal indices m and m' are the same. Between two TE modes with different radial indices in a long cavity ($d \gg a$), there is little coupling because they are widely separated in frequency (criterion 2)). If the modes have the same radial indices but different axial indices, $k_\perp \gg k_z$ yielding $Q_{hh}^{\alpha\beta} \gg Q_{hh}^{\alpha\alpha}$ and there is very little cross-coupling by criterion 1). This is true for lower order axial modes that are of interest in gyrotron cavities. In a cavity where $d \approx a$ both the radial and axial indices of the two modes have to be different to meet criterion 2) but such a choice of indices makes the crossc-coupling $Q_{hh}^{\alpha\beta} = \infty$ (in a completely enclosed cavity). Finally, there are no $TE_{mnp} - TM_{mn'p'}$ mode pairs which satisfy both criteria for coupling.

Disruption of symmetry in the azimuthal, radial, or axial directions removes the effective $\delta_{mm'}$, $\delta_{nn'}$, and $\delta_{pp'}$ terms in the Q-factor expressions, but the $Q_{hh}^{\alpha\beta}$ are generally substantially larger than the $Q_{hh}^{\alpha\alpha}$.

To demonstrate mode cross-coupling through ohmic effects more clearly, the rectangular cavity shown in Fig. 3 is used with dimensions of $a = 0.017\,83$ m, $b = 0.008$ m, $c = b/100$, and $d = 0.04$ m. The height of the waveguide is much smaller than that of the cavity to suppress the external coupling. The dominant mode in the waveguide is TE_{10} which primarily excites the TM_{111} cavity mode near 20.86 GHz. Fig. 6 shows the effects of ohmic cross coupling from the TM_{111} mode into the TE_{111} mode. The energy in the TE_{111} mode is compared for cases with and without the cross-coupling Q-factors ($Q_{hh}^{\alpha\beta}$). The choice of cavity dimensions results in degenerate frequencies for the TM_{111} and TE_{111} modes, and $\frac{f_{TE_{111}}}{Q_{hh}^{TE_{111}-TE_{111}}} \approx \frac{f_{TM_{111}}}{Q_{hh}^{TE_{111}-TM_{111}}}$. The cross-coupling ohmic Q-factors clearly cause a shift in the frequency where the energy in the TE_{111} mode is at its peak.

Fig. 7 shows a coupled (complex) cavity gyrotron [9]. The gyrotron cavity consists of the main cavity strongly coupled to a filtering cavity. The waveguide is used to couple power out of the main cavity. The main cavity has a dense modal spectrum while the filtering cavity has a rarefied modal spectrum. The filtering cavity is used to enhance selected resonances. The gyrotron electron beam excites fields in both the main and filtering cavities. For optimal gyrotron oscillation, the electron beam requires fields of similar spatial structure in the two cavities. Because the two cavities have different radial dimensions, to match the fields at the junction they are operated with the same azimuthal modal index but different radial indices. This is achieved by designing the cavity dimensions such that the TE_{mn} and TE_{mq} resonant mode frequencies in the cavities are approximately the same by using the relation

$$\frac{r_1}{r_2} = \frac{x_{m,n}}{x_{m,q}}$$

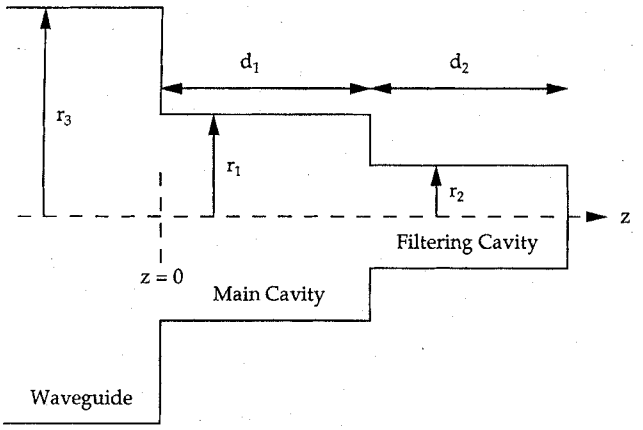

Fig. 7. Cross section of a coupled (complex) gyrotron cavity.

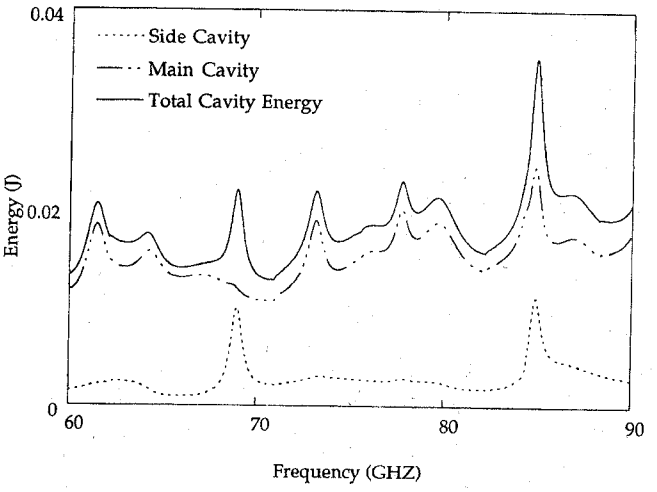

Fig. 8. Energy spectrum for the coupled (complex) cavity.

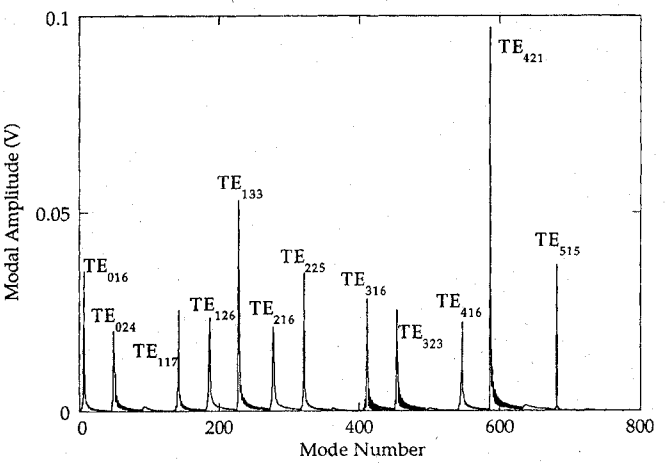

Fig. 9. Modal content of the 84.8 GHz resonance in Fig. 7.

where $x_{m,n}$ and $x_{m,q}$ are the n'th and q'th roots of the equation $(J'_m(x) = 0)$. An 85 GHz oscillator is designed with the dimensions $r_1 = 0.5288$ cm, $r_2 = 0.3192$ cm, $r_3 = 0.5488$ cm, $d_1 = 1.1996$ cm, and $d_2 = 0.4253$ cm. The cavity dimensions are chosen such that the TE_{421} mode in the main cavity and the TE_{411} mode in the filtering cavity have resonances near 84.8 GHz.

The power in the incident waves (all propagating waveguide modes) through the waveguide was held constant, normalized to one watt at all frequencies in all the modes. Twenty-one transverse TE_{mn} modes were used in the waveguide and 800 TE_{mnp} modes were used in the cavity. Fig. 8 shows the energy stored in the main cavity, energy stored in the filtering cavity, and their sum as a function of frequency. The main cavity has many resonances in the frequency window shown here, but the filtering cavity has just two resonances, and the resonant frequencies of the main and filtering cavities coincided at 84.8 GHz to produce a significant overall resonance in the cavity structure. Fig. 9 shows the modal amplitudes of each of the modes in the main cavity at 84.8 GHz (the frequency of strongest resonance in the overall structure). The TE_{421} mode has the largest amplitude but many other modes are present, indicating significant mode coupling. Aside from the TE_{421} mode, all the cavity modes which have resonant frequencies near 84.8 GHz are strongly excited.

IV. Conclusion

A mode-matching method used to compute the fields, modal amplitudes, and admittances of a gyrotron cavity is presented. The method has the advantage that it can compute the amplitudes of individual modes in the cavity as well as the total fields. Because of this feature, this method is particularly well suited to the study of gyrotron operation. The formulation is computer coded, and results from benchmark cases indicate the correctness of the results. The results for the case of the single circular cavity coupled out by a circular waveguide indicate the degree of mode coupling through external radiation losses and ohmic wall losses. The rectangular cavity example demonstrates the ohmic cross-coupling between two cavity modes. Results from the coupled (complex) cavity case demonstrate that the two-cavity design selectively enhances a particular mode. The analytical formulation presented here can be modified to include more complicated structures such as tapered wall cavities, waveguides and co-axial cavities. The formulation is also suitable for inclusion of a gyrotron electron beam, which is the subject of ongoing work.

Appendix

For the TE_{mnp} modes in a cylindrical cavity, the eigenvectors are given as

$$\vec{E}_\alpha = \frac{1}{C_\alpha}\left\{-\hat{\rho} m k_\alpha J_m\left(x'_{mn}\frac{\rho}{a}\right)\frac{\sin m\phi}{\rho}\sin\frac{p\pi z}{d} - \hat{\phi} k_\alpha \frac{x'_{mn}}{a} J'_m\left(x'_{mn}\frac{\rho}{a}\right)\cos m\phi \sin\frac{p\pi z}{d}\right\}.$$

In the waveguide, the electric field eigenvectors for the TE modes are given as

$$\vec{E}_w = \frac{1}{C_w}\left\{\hat{\rho} m J_m\left(x'_{mn}\frac{\rho}{b}\right)\frac{\sin m\phi}{p} + \hat{\phi}\frac{x'_{mn}}{b} J'_m\left(x'_{mn}\frac{\rho}{b}\right)\cos m\phi\right\}.$$

Here C_α and C_w are normalization constants, x'_{mn} is the n'th zero of J'_m and x_{mn} is the n'th zero of J_m, a and b are the radii of the cavity and waveguide, respectively. The coupling coefficients are given as

$$\gamma_{\alpha s} = -\frac{2\pi\delta_{mm'}}{\epsilon_m C_\alpha C_w}\frac{p\pi}{d}\left\{\frac{x'_{mn}x'_{m'n'}}{ab}A^1_{m,m',n,n'}(\rho) + mm'(1-\delta_{m0})A^2_{m,m',n,n'}(\rho)\right\}$$

where the unprimed indices are for cavity modes and primed indices are for waveguide modes. Similarly

$$\beta_{\lambda s} = -\frac{2\pi\delta_{mm'}}{C_\lambda C_w k_\lambda \epsilon_m}\left\{\frac{x'_{mn}x'_{m'n'}}{ab}A^1_{m,m',n,n'}(\rho) + mm'(1-\delta_{m0})A^2_{m,m',n,n'}(\rho)\right\}.$$

The Q factors are computed from (14). The integrals in (14) are as follows

$$\begin{aligned}&\int_S \vec{H}_\alpha\cdot\vec{H}_\beta ds\\ &= 4\frac{p\pi}{d}\frac{p'\pi}{d}\frac{\pi\delta_{mm'}}{C_\alpha C_\beta\epsilon_m}\\ &\times\left\{\frac{x'_{mn}x'_{m'n'}}{ab}B^1_{m,m',n,n'}(\rho)+mm'(1-\delta_{m0})B^2_{m,m',n,n'}(\rho)\right\}\\ &+\frac{2\pi\delta_{mm'}}{C_\alpha C_\beta}\frac{d}{\epsilon_p\epsilon_m}\delta_{pp'}J_m(x'_{mm})J_m(x'_{mn'})\\ &\times\left\{m^2\frac{p^2\pi^2}{d^2}\left(\frac{1-\delta_{m0}}{a}\right)+a\left(k_\alpha^2-\frac{p^2\pi^2}{d^2}\right)\left(k_\beta^2-\frac{p^2\pi^2}{d^2}\right)\right\}.\end{aligned}$$

Here ϵ_p and ϵ_m are the Neumann factors ($\epsilon_p = 1$ for $p = 0$, and $\epsilon_p = 1$ for $p \neq 0$); the unprimed indices correspond to the $\vec{H}_\alpha$, and the primed indices correspond to $\vec{H}_\beta$. Similarly

$$\begin{aligned}&\int_S \vec{H}_\alpha\cdot\vec{G}_\lambda ds\\ &= 4\frac{p\pi}{d}\frac{1}{k_\lambda}\frac{\pi\delta_{mm'}}{C_\alpha C_\lambda\epsilon_m}\\ &\times\left\{\frac{x'_{mn}x'_{m'n'}}{ab}B^1_{m,m',n,n'}(\rho)+mm'(1-\delta_{m0})\right.\\ &\quad\left.\times B^2_{m,m',n,n'}(\rho)\right\}\\ &+2\frac{d}{\epsilon_p}\delta_{pp'}\frac{\pi\delta_{mm'}}{C_\alpha C_\lambda\epsilon_m}\frac{J_m(x'_{mm})J_m(x'_{mn'})}{k_\lambda}\\ &\times\left\{\frac{mm'}{a}\frac{p\pi}{d}-a\frac{p'\pi}{d}\left(k_\alpha^2-\frac{p^2\pi^2}{d^2}\right)\right\}\end{aligned}$$

where the unprimed indices correspond to $\vec{H}_\alpha$ and primed indices correspond to $\vec{G}_\lambda$

$$\begin{aligned}&\int_S \vec{G}_\lambda\cdot\vec{G}'_\lambda ds = \frac{4\pi\delta_{mm'}}{C_\lambda C'_\lambda k_\lambda k'_\lambda\epsilon_m}\\ &\times\left\{\frac{x'_{mn}x'_{m'n'}}{ab}B^1_{m,m',n,n'}(\rho)+mm'(1-\delta_{m0})\right.\\ &\quad\left.\times B^2_{m,m',n,n'}(\rho)\right\}\\ &+2\frac{d}{\epsilon_p}\delta_{pp'}\frac{\pi\delta_{mm'}}{C_\lambda C'_\lambda k_\lambda k'_\lambda\epsilon_m}\frac{J_m(x'_{mm})J_m(x'_{mm'})}{k_\lambda}\\ &\times\left\{\frac{mm'}{a}+a\frac{p\pi}{d}\frac{p'\pi}{d}\right\}\end{aligned}$$

where the unprimed indices correspond to $\vec{G}_\lambda$ and primed indices correspond to $\vec{G}'_\lambda$. Here

$$A^1_{m,m',n,n'}(\rho) = \int_0^b f^1_{m,m',n,n'}(\rho)\rho d\rho,$$

$$A^2_{m,m',n,n'}(\rho) = \int_0^b f^2_{m,m',n,n'}(\rho)\frac{d\rho}{\rho}$$

and

$$B^1_{m,m',n,n'}(\rho) = \int_0^a f^3_{m,m',n,n'}(\rho)\rho d\rho,$$

$$B^2_{m,m',n,n'}(\rho) = \int_0^a f^4_{m,m',n,n'}(\rho)\frac{d\rho}{\rho}$$

and where

$$f^1_{m,m',n,n'}(\rho) = J'_m\left(x'_{mn}\frac{\rho}{a}\right)J'_{m'}\left(x'_{m'n'}\frac{\rho}{b}\right),$$

$$f^2_{m,m',n,n'}(\rho) = J_m\left(x'_{mn}\frac{\rho}{a}\right)J_{m'}\left(x'_{m'n'}\frac{\rho}{b}\right)$$

and

$$f^3_{m,m',n,n'}(\rho) = J'_m\left(x'_{mn}\frac{\rho}{a}\right)J'_{m'}\left(x'_{m'n'}\frac{\rho}{a}\right),$$

$$f^4_{m,m',n,n'}(\rho) = J_m\left(x'_{mn}\frac{\rho}{a}\right)J_{m'}\left(x'_{m'n'}\frac{\rho}{a}\right).$$

In (18) and (19), the coefficient matrix elements are given as

$$A_{\alpha,\varphi} = \frac{-k_\alpha\eta(\omega)}{k_\alpha^2-\frac{\omega^2}{c^2}}\frac{j\omega\varepsilon}{k_\varphi}\frac{1}{Q^{\alpha\varphi}_{hh}\delta}f_\varphi;$$

$\alpha,\varphi = 1,$ total number of cavity modes used

$$B_{\alpha,s} = \frac{k_\alpha}{k_\alpha^2-\frac{\omega^2}{c^2}}\left(\gamma_{\alpha,s}-\sum_\varphi\frac{\eta(\omega)}{Q^{\alpha\varphi}_{hg}\delta}\frac{\beta_{\varphi,s}}{j\omega\mu}\right);$$

$\alpha,\varphi = 1,$ total number of cavity modes used

$s = 1,$ total number of waveguide modes used

$$C_{r,\alpha} = \frac{j\omega\varepsilon}{k_\alpha}\left[\gamma_{\alpha,r}+j\sum_\lambda\beta_{\lambda,r}\frac{\eta(\omega)}{\omega\mu}\frac{1}{Q^{\lambda\alpha}_{hg}\delta}\right];$$

$r = 1,$ total number of waveguide modes used

$\alpha,\lambda = 1,$ total number of cavity modes used

$$D_{r,s} = \left[\left\{\sum_\alpha\sum_\lambda\beta_{\alpha,r}\beta_{\lambda,s}\frac{\eta(\omega)}{\omega^2\mu^2}\frac{1}{Q^{\alpha\lambda}_{gg}\delta}\right\} - j\left\{\sum_\alpha\frac{\beta_{\alpha,r}\beta_{\alpha,s}}{\omega\mu}\right\}\right];$$

$r,s = 1,$ total number of waveguide modes used

$\alpha,\lambda = 1,$ total number of cavity modes used.

Equations (17)–(19) are solved as

$$(v^-) = ((D)+(Y_w))^{-1}[(C)(f)+((D)-(Y_w))(v^+)]$$

where

$$\begin{aligned}(f) = &\{(I)-(A)+(B)((D)+(Y_w))^{-1}(C)\}^{-1}(B)\\ &\times\{(I)-((D)+(Y_w))^{-1}((D)-(Y_w))\}(v^+).\end{aligned}$$

Here (Y_w) is a diagonal matrix with waveguide modal admittances as its elements, and (I) is the identity matrix.

REFERENCES

[1] R. F. Harrington, *Time-Harmonic Electromagnetic Fields*. New York: McGraw-Hill, ch. 8, 1961.

[2] J. C. Slater, *Microwave Electronics*. New York: Van Nostrand, ch. 3, 1950.

[3] T. Teichmann and E. P. Wigner, "Electromagnetic field expansions in loss-free cavities excited through holes," *J. Appl. Phys.*, vol. 24, pp. 262–267, Mar. 1953.

[4] K. Kurokawa, "The expansions of electromagnetic fields in cavities," *IRE Trans. Microwave Theory Tech.*, vol. MTT-6, pp. 178–187, Apr. 1958.

[5] A. K. Bhattacharyya, "Multimode moment method formulation for waveguide discontinuities," *IEEE Trans. Microwave Theory Tech.*, vol. 42, pp. 1567–1571, Aug. 1994.

[6] H. Auda and R. F. Harrington, "A moment solution for waveguide junction problems," *IEEE Trans. Microwave Theory Tech.*, vol. MTT-31, pp. 515–519, July 1983.

[7] M. Leong, P. S. Kooi, and P. Chandra, "A new class of basis functions for the solution of the E-plane waveguide discontinuity problem," *IEEE Trans. Microwave Theory Tech.*, vol. MTT-35, pp. 705–709, Aug. 1987.

[8] D. K. Cheng, *Fundamentals of Engineering Electromagnetics*. Reading: Addison-Wesley, ch. 10, 1993.

[9] V. G. Pavelev, S. E. Tsimring, and V. E. Zapevalov, "Coupled cavities with mode conversion in gyrotrons," *Int. J. Electronics*, vol. 63, pp. 379–391, 1987.

[10] A. Wexler, "Solution of waveguide discontinuities by modal analysis," *IEEE Trans. Microwave Theory Tech.*, vol. MTT-15, p. 508, 1967.

[11] J. M. Neilson, P. E. Latham, M. Caplan, and W. G. Lawson, "Determination of the resonant frequencies in a complex cavity using the scattering matrix formulation," *IEEE. Trans. Plasma Sci.*, vol. 37, p. 1165, 1989.

[12] R. J. Temkin, "Analytic theory of a tapered gyrotron resonator," *Int. J. Infrared and Millimeter Waves*, vol. 2, pp. 629–649, 1981.

[13] R. E. Collin, *Field Theory of Guided Waves*. Piscataway, NJ: IEEE Press, ch. 5, 1991.

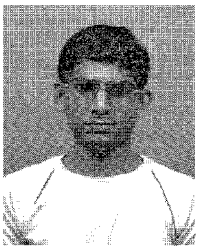

Vasu Kasibhotla (S'90) received the B.Tech. degree in electrical engineering from Regional Engineering College (Warangal), India in 1986, and the M.S. degree in electrical engineering from Florida State University in 1990. Since 1991 he has been a Ph.D. candidate in the Electrical Engineering department at the University of Southern California.

His research interests are in the areas of microwave engineering, electromagnetics, and high power microwave sources.

Mr. Kasibhotla is a member of the American Physical Society.

Alan H. McCurdy (M'92) received the B.S. degree in chemical engineering from Carnegie-Mellon University, Pittsburgh, PA, in 1981, and the B.S. in physics from the same institution in 1982. He received the Ph.D. degree in applied physics from Yale University, New Haven, CN, in 1987.

He worked in the Electronics Science and Technology Division at the Naval Research Laboratory from 1985 until 1988. Since 1988 he has been on the electrical engineering faculty at the University of Southern California and is currently an Associate Professor. His current interests include short pulse microwave generation and mode locking of microwave devices.

Dr. McCurdy is a member of the American Physical Society. He received the Simon Ramo Award in 1988 and the Northrop Junior Faculty Research Award in 1992 for his work on phase and mode control in gyrotron oscillators.